

# Machine-learned Adaptive Switching in Voluntary Lower-limb Exoskeleton Control: Preliminary Results

Pouria Faridi, Javad K. Mehr, *Student Member, IEEE*, Don Wilson, Mojtaba Sharifi, *Member, IEEE*, Mahdi Tavakoli, *Senior Member, IEEE*, Patrick M. Pilarski, *Senior Member, IEEE*, and Vivian K. Mushahwar, *Member, IEEE*

**Abstract**— Lower-limb exoskeletons utilize fixed control strategies and are not adaptable to user’s intention. To this end, the goal of this study was to investigate the potential of using temporal-difference learning and general value functions for predicting the next possible walking mode that will be selected by users wearing exoskeletons in order to reduce the effort and cognitive load while switching between different modes of walking. Experiments were performed with a user wearing the Indego exoskeleton and given the authority to switch between five walking modes that were different in terms of speed and turn direction. The user’s switching preferences were learned and predicted from device-centric and room-centric measurements by considering similarities in the movements being performed. A switching list was updated to show the most probable future next modes to be selected by the user. In contrast to other approaches that either can only predict a single time-step or require intensive offline training, this work used a computationally inexpensive method for learning and has the potential of providing temporally extended sets of predictions in real-time. Comparing the number of required manual switches between the machine-learned switching list and the best possible static lists showed an average decrease of 42.44% in the required switches for the machine-learned adaptive strategy. These promising results will facilitate the path for real-time application of this technique.

## I. INTRODUCTION

Powered lower-limb exoskeletons provide assistance to their users and have different active joints that can be controlled by the users, depending on the implemented control strategy for the device [1], [2]. What makes these exoskeletons beneficial for rehabilitation and gait restoration research is their capability of tracking the desired motions presented to them with high accuracy, collecting data of different joint motions with their built-in sensors that can be used as feedback, and providing different levels of assistance to users with a variety of conditions such as people with complete

spinal cord injury (SCI) (no motor function) and incomplete SCI (limited motor function) [3].

The ultimate goals of many research avenues in this domain are: 1) taking into account users’ intention 2) reducing the effort needed to perform tasks and 3) making the orthosis adaptive to the users’ need in a safe manner. To this end, many control strategies have been designed and tested experimentally. Generally, there are three main areas of focus for designing control strategies for exoskeletons: high-level, mid-level and low-level control [4], [5]. The main focus of this work is on high-level control and as a result, the remainder of this introduction is allocated to the high-level control concept.

A high-level controller can be seen as a perception and motion planning layer [6] that characterizes the overall status or behavior of the robotic device. Both knowledge of the environment and user-dependent measurements (such as ground reaction forces, joint torques, joint angles, etc.) can be used as the inputs to the high level controller, while the output is expected to be a specific mode of walking [5]. The modes available on a control system are predefined modes. These modes are designed based on the needs of the users. They can contain different speeds and lengths of walking [7], various tasks such as stair ascending/descending [7]–[9], sit-to-stand and stand-to-sit transitions [7], [10] and also different states of over-ground walking [11]. In this regard, selecting the user’s intended next mode can be seen as the major concern of high-level controllers, especially when a variety of modes are present.

In a recent review [5], high-level controllers were divided into 4 main categories as: brain-computer interfaces, movement recognitions, terrain detections and manual user inputs. The first category, which mostly uses electroencephalography (EEG) recordings from the brain [12]–[15], faces many practical issues. Artifact removal,

\*Research supported by the Canadian Institutes of Health Research, Canada Foundation for Innovation, Alberta Ministry of Advanced Education, the grant of the Alberta Ministry of Jobs, Economy and Innovation to the Centre for Autonomous Systems in Strengthening Future Communities.

P. Faridi is with the Neuroscience and Mental Health Institute, University of Alberta, Edmonton, Alberta, Canada (corresponding author; e-mail: [Pfaridi@ualberta.ca](mailto:Pfaridi@ualberta.ca))

J. K. Mehr is with the Department of Electrical and Computer Engineering and Department of Medicine, University of Alberta, Edmonton, Alberta, Canada (e-mail: [Khodaeim@ualberta.ca](mailto:Khodaeim@ualberta.ca))

D. Wilson is with the Department of Medicine, University of Alberta, Edmonton, Alberta, Canada (email: [don4@ualberta.ca](mailto:don4@ualberta.ca))

M. Sharifi is with the Department of Mechanical Engineering, San Jose State University, San Jose, California 95192-0087 (e-mail: [sharifi3@ualberta.ca](mailto:sharifi3@ualberta.ca))

M. Tavakoli is with the Department of Electrical and Computer Engineering, University of Alberta, Edmonton, Alberta, Canada T6G 1H9 (e-mail: [Mahdi.tavakoli@ualberta.ca](mailto:Mahdi.tavakoli@ualberta.ca))

P. M. Pilarski is with the Alberta Machine Intelligence Institute (Amii), and Department of Medicine, Division of Physical Medicine and Rehabilitation, University of Alberta, Edmonton, Alberta, Canada T6G 2E1 (e-mail: [Pilarski@ualberta.ca](mailto:Pilarski@ualberta.ca))

V. K. Mushahwar is with the Department of Medicine, Division of Physical Medicine and Rehabilitation, and the Neuroscience and Mental Health Institute, University of Alberta, Edmonton, Alberta, Canada T6G 2R3 (e-mail: [Vivian.Mushahwar@ualberta.ca](mailto:Vivian.Mushahwar@ualberta.ca))

All authors are with the Sensory Motor Adaptive Rehabilitation Technology (SMART) Network, University of Alberta, Edmonton, Alberta, Canada T6G 2R3

requirement of high concentration by the user, the lengthy procedure of preparing the EEG electrodes, and losing accuracy over time are among those issues [5], [16].

Another group of strategies (movement recognitions) aims to determine the desired mode of walking by relying on the user’s body movements and forces. Examples are studies focused on threshold crossing techniques [17], [18], and machine learning algorithms, mostly supervised learning, to classify sensor values for specific modes [20], [21]. These systems either require a precise threshold setting or a high amount of recorded data for their training sets [22].

The third category, using sensors or cameras such as infrared distance sensors [23], [24], head-mounted cameras [25], and chest-mounted RGB camera systems [26], has shown promising results. Nonetheless, if implemented independently of other high level control categories, its usage is limited to modes that are only environment-dependent.

The last category (manual user input) works directly through user commands, either with switch buttons or voice-control [5], [7], [27]. Using switch buttons is the most commonly used method of high-level control [5] because of the simplicity of its implementation, capacity for adding more modes and less susceptibility to errors. Despite the benefits of push-button systems, they have several drawbacks. Using a single switch requires high transition times to toggle between modes and also a high number of required switching actions for a switching instance. Using a panel of switches for each mode also limits the capacity of adding many modes. Therefore, both of these push-button strategies make the user feel uncomfortable, reduce the speed of tasks, and require a high degree of mental concentration, thus increasing the chance of errors [5].

Considering all the aforementioned control approaches, this work aimed to 1) reduce the switching-related problems in high-level control of lower-limb exoskeletons while using the switch-button method, and 2) increase the users’ confidence in the device by employing reinforcement learning techniques and predicting users’ intention. The goal was to design an adaptive switching controller that updates the order of modes in a pre-designed switching list at each time-step based on the user’s previous activity and locational information. This information was used to predict the most probable next mode that the user would select, and suggest that mode as the first mode in the switching list. If successful, this will make the switching actions easier and faster, and improve the use of exoskeletons for upright mobility.

## II. METHODS

### A. Robotic Platform

The powered orthosis used in this study was the Indego lower-limb exoskeleton (Parker Hannifin Corporation, Cleveland, Oh, USA) with powered hip and knee joints (by brushless DC motors) [28]. Joints were also equipped with a potentiometer to provide the actual angles at each time-step. The performance of the exoskeleton was controlled by on-board components, connected to a laptop with an Intel Core i7 CPU via USB. The control strategy was designed in Real-time Desktop Simulink environment of MATLAB (The MathWorks, Inc., Natick, MA, USA) and communicated with

the exoskeleton system through the CAN interface (Vector VN1610).

A walker was equipped with additional components. A 5-button switch panel was designed and mounted on the right side of the walker for switching purposes on the part of the user. To acquire locational information, 3 GARMIN LIDAR-Lite v4 LiDAR (Light Detection and Ranging) sensors were installed on 3 sides of the walker to provide distance to objects around. The system received the external signals and operated at 50Hz. The platform setup can be seen in Fig. 1.

### B. Experimental Procedures

The experiments were performed in 2 different scenarios. For each scenario, the user (neurologically-intact, male, 24 years old and experienced in working with the exoskeleton) had the authority to switch between 5 available walking modes as: 3 different speeds (slow, normal and fast) and 2 turning directions (left and right) using the switch button panel. For the purposes of this study, a switching panel consisting of 5 buttons was designed and used to assess the core capabilities of the machine learning algorithm on predicting the next

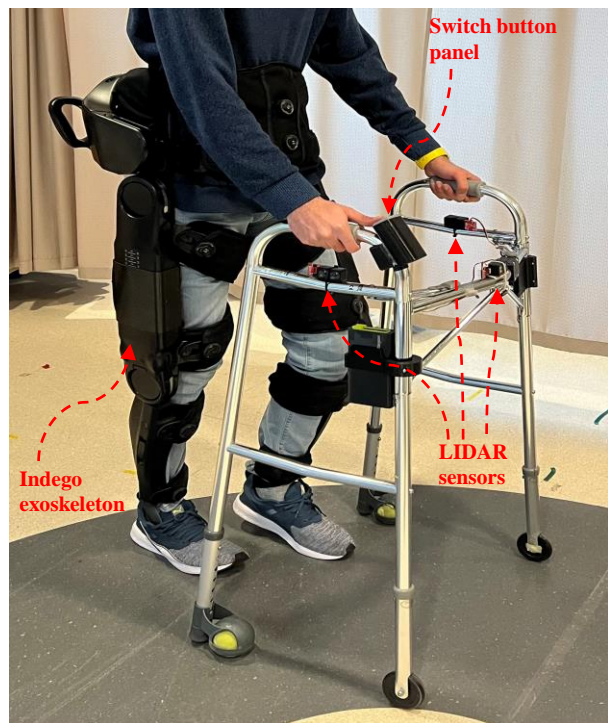


Figure 1. A study investigator wearing the exoskeleton with a walker equipped with a switch button panel and distance measurement sensors.

TABLE I. CHARACTERISTICS OF DESIGNED WALKING MODES

Walking mode	Walking characteristics	
	Speed (m/s)	Stride length (m)
Slow speed	0.23	0.875
Normal speed	0.31	1.050
Fast speed	0.39	1.125
Turning left/right	0.15	0.725

❖ Colored arrows are indicative of the modes being used as: **Slow speed**, **Normal speed**, **Fast speed**, **Left turn**, **Right turn**

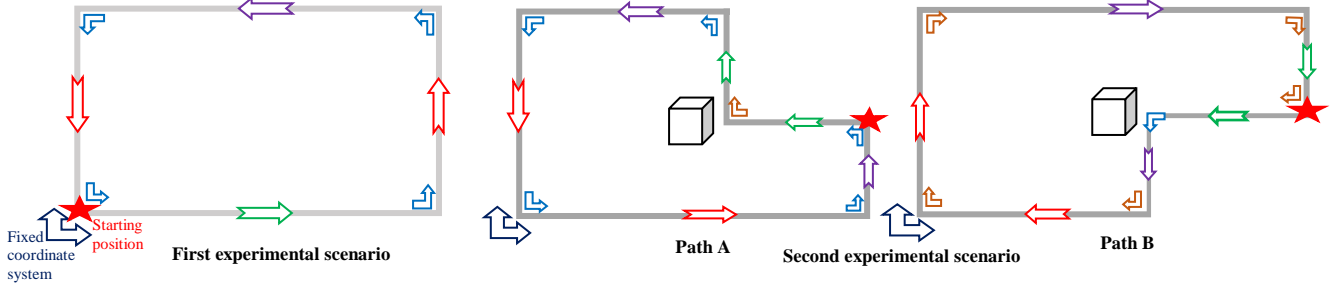


Figure 2. Experimental design scenarios. In the first scenario (left image) a rectangular path was walked by the user, using different walking modes in the directions specified on the image. This pattern was repeated for six times. In the second scenario, the user had the authority to select between two available paths (A,B) for each round of walking. A total of 11 rounds were walked by the user in the order of: A,A,B,A,B,B,B,A,A,B,B. A fix coordinate system was used at the bottom left of the experimental areas to calculate the position of the user at each time-step based on the speed of walking and the time spent in a specific mode and specific direction. The red star indicates the starting position for each scenario.

walking mode, and avoid the delays upon mode switching while collecting experimental data for the machine learning algorithm. However, using a separate button for each mode is not a scalable solution when there is a larger number of modes to switch to.

After a mode was selected by the user, the desired trajectory of that mode was implemented by the designed controller using central pattern generator (CPG) concepts [18], [29] in which specific pre-defined frequency and amplitude of each mode were passed through the differential equations of motion, and a reference trajectory was updated for each joint to allow a smooth transition between walking modes. The built-in proportional-derivative (PD) tracking system of the Indego exoskeleton with modified gains [30] was used to track the desired trajectories. The characteristics of the designed walking modes are shown in Table I. These were chosen based on the mean gait speed of people with SCI walking with the Indego exoskeleton [31].

In the first experimental scenario, the user walked through a rectangular path (4.5m \* 5m) 6 times (rounds), using the walking modes as shown in Fig. 2. This scenario was designed to test the core machine learning capabilities in prediction and learning. In the second scenario, the user had the authority to select between two different paths, separated by an obstacle, at each round when he reached the starting position (Fig. 2). A total of 11 rounds (from starting position, back to the starting position) were walked by the user, with an arbitrary order of choosing between the two available paths. This scenario was designed with the goal of testing the capability of the designed machine learning strategy in differentiating between different paths and providing reasonable mode suggestions upon approaching an obstacle.

### C. Machine Learning Strategy

The machine learning strategy implemented in this work was based on a technique from reinforcement learning called general value functions (GVFs) [32]. GVFs are value functions with the ability of representing temporally extended predictions of arbitrary signals [33]–[34] and have been implemented to design adaptive and autonomous controllers in myoelectric prostheses [35]–[38]. In this study, GVFs were used to provide anticipatory knowledge on the next possible walking mode to be selected by the user from a switching list in order to minimize the number of manual switches needed to

be performed by the user. The proposed machine learning strategy was implemented on all of the collected data, in an offline setup, for the purpose of preliminary verifications.

Position and distance information was used to anticipate the levels of mode activities. Signals from the 3 LiDAR sensors in addition to the position of the user in the 2D x-y plane (computed mathematically by considering a reference coordinate system and the time spent in each mode along with the speed of that mode) formed the state-space ( $s$ ) of the system (Fig. 3). LiDAR signals were able to provide information on reaching to an obstacle. These five signals were then passed through a function approximation method called Selective Kanerva coding (SKC) [39] to provide a binary vector. The resultant binary vector, called feature vector ( $x$ ), contained 15000 elements in which the 650 closest elements to each state were active at all times. For algorithm details and parameters' selection please refer to Dalrymple et al. [40].

An activation level ( $c$ ) was also defined for each mode. The walking mode selected by the user at each time-step was considered the active mode, given a value of  $c_j=1$  while all other modes received a value of  $c_j=0$  ( $j \equiv$  number of modes). One GVF weight vector  $w_j$  was also initialized at the beginning of each experiment for each mode that was updated at each learning time-step (Algorithm 1). The inner product of the

---

#### Algorithm 1 GVF prediction and learning with TD( $\lambda$ )

---

**Initialize**  $w, e, s, x$

**Repeat** every time step:

**Observe** next state  $s$

$x' \leftarrow SKC(s)$

**For** all modes  $j$  **do**:

**Observe** mode activity signal  $c_j$

$\delta \leftarrow c_j + \gamma w_j^T x' - w_j^T x$

$e_j \leftarrow \min(\lambda e_j + x, 1)$

$w_j \leftarrow w_j + \alpha \delta e_j$

$p_j \leftarrow w_j^T x'$

$x \leftarrow x'$

**Rank** the modes in the switching list

---

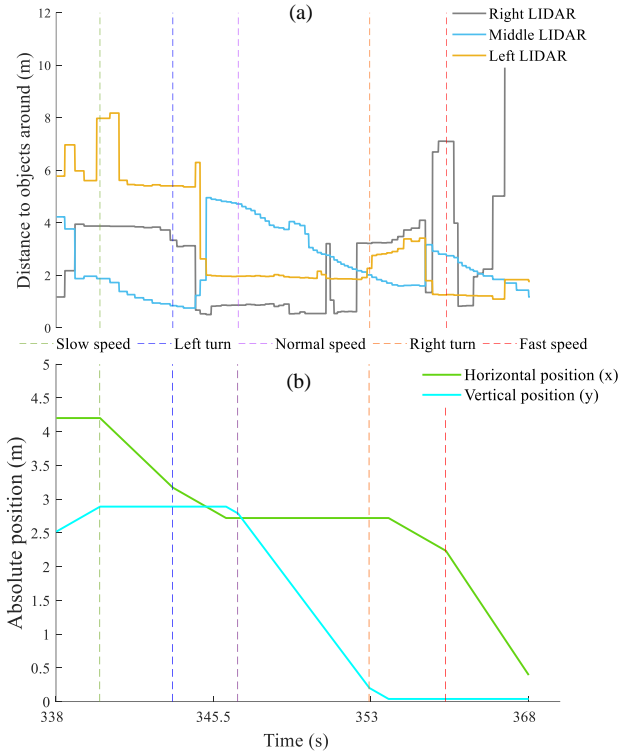


Figure 3. Signals used in the state-space of the system for a sample of recorded data during the second experimental scenario (path B). The selected modes by the user are specified with dashed lines at the switching instances for both images. (a) The signals from the LiDAR sensors. These 3 signals were used to monitor the distance of the user from obstacles. (b) The absolute position of the user in the 2D space, computed mathematically at each time-step (0.02 sec), using a reference fixed coordinate system and related mathematical relationships. The signals from the LiDAR sensors and the computed absolute space were used for identifying similarities in the modes being selected at specific positions. The horizontal axis for (a) and (b) represents the specific time these signals were taken during walking.

weight vector and the feature vector (from SKC) was introduced as the GVF prediction value ( $p_j$ ) for each mode. These GVF predictions were then ranked in the switching list based on their relative magnitude in a descending order, with the current active mode being ranked last, regardless of its prediction value.

GVF predictions ( $p_j$ ) and their weight vectors were then updated at each time-step using the temporal-difference learning method ( $TD(\lambda)$ ) presented in Algorithm 1, in which a TD error signal ( $\delta$ ) was formed as the difference between the discounted future prediction and the prediction for the current state, plus the current mode activation signal ( $c_j$ ). Replacing eligibility traces ( $e_j$ ) were then used [41] with TD error ( $\delta$ ) to update the weight vectors. For more information on TD learning please see [36], [42].

The discounting factor used in updating the TD error ( $\delta$ ) was set to  $\gamma=0.992$  for all modes and  $\alpha=0.001$  was used for weight vector updates as the step-size parameter, based on a comprehensive trial and error. The bootstrapping parameter in the replacing eligibility traces update was set to  $\lambda=0.9$ , as is often standard [40].

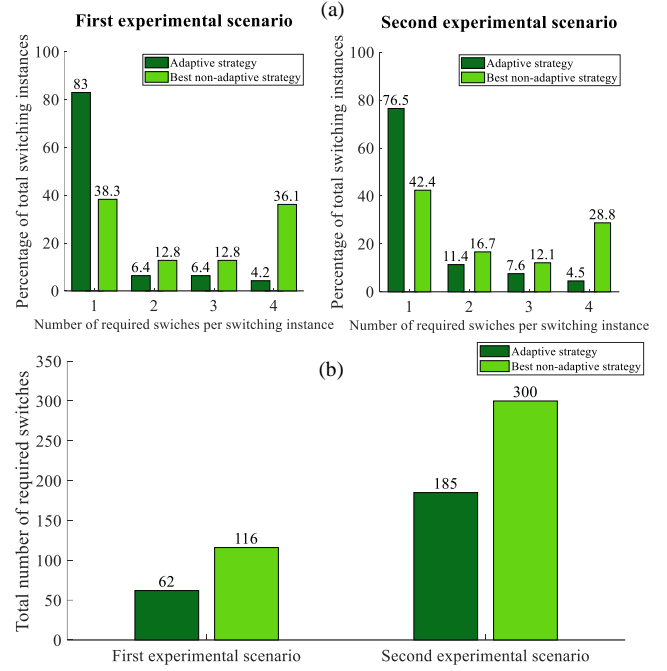


Figure 4. Number of switches required using a single switch button under the adaptive and the best possible non-adaptive strategy, computed post-hoc. (a) The percentage of times where 1,2,3 or 4 switches were needed to reach to the user's desired mode at each switching instance for the first (left) and second (right) experimental scenarios. (b) Total number of required switches using the two strategies under the two experimental scenarios.

### III. RESULTS

A comparison of the number of instances in which the next selected mode by the user was ranked first, second, third and fourth in the switching list for both experimental scenarios under adaptive and best possible non-adaptive control is shown in Fig. 4a. The comparison is based on the use of a single switch button to transition to the desired mode. In the adaptive controller strategy, the system was able to quickly adjust the switching list based on the user preferences and with regards to locational and positional information provided to the system. In the first experimental scenario (Fig. 4a, left), it can be seen that the system was able to predict correctly the next mode at the times of mode switching by the user and rank it as the first in the switching list for 82.98% (39 out of 47) of times, while all other switches that were not ranked first were limited to the first and second rounds of walking along the rectangular path. However, using the best non-adaptive strategy, as computed separately for each experimental scenario, showed that in only 18 out of 47 switching instances (38.3% of times) one switching action was required from user and the remaining selections required two or more switching actions. Switching numbers for the second experimental scenario (Fig. 4a, right), which was more complicated and had two different paths, showed that in 76.52% of instances (101 out of total 132 switching instances) the next selected mode was ranked first, while this number for the fixed-list strategy was 34.1% lower (42.42% of instances, 56 out of 132).

The total number of required switches to perform the tasks under each strategy is shown in Fig. 4b. For the first experimental scenario, the total number of required switches decreased by 46.55% for the adaptive strategy in comparison

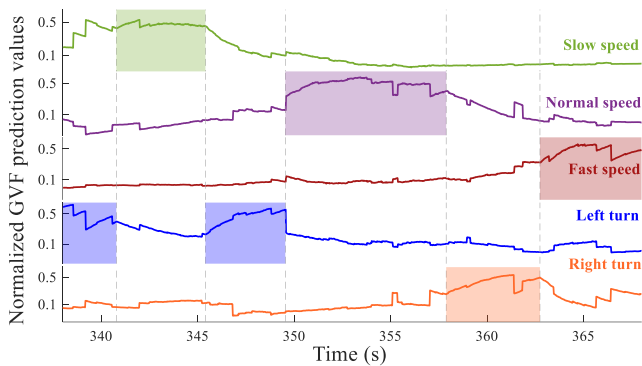


Figure. 5 Normalized GVF prediction values for a sample of recorded data during the second experimental scenario (path B) after 4 rounds of walking in the order of A, A, B and A. Solid lines show the predictions for each mode activation level and dashed lines represent the user's switching actions from the previous active mode (left side of the dashed lines) to the next intended mode (right side of the dashed lines). Modes in the switching list were ranked at each time-step (0.02 sec) based on their GVF prediction value in descending order, except for the active mode that always was ranked least, regardless of its GVF value.

to the best computed non-adaptive case. Also, the second experimental scenario showed a 38.33% decrease in the number of total switches upon using the adaptive strategy relative to the best non-adaptive strategy which was also task-specific. These advantages are also expected to be more appreciated upon increasing the number of available modes in the switching list.

An example of the GVFs predictions as an indication of the expected mode activation levels for a subset of collected data from the second experimental scenario is depicted in Fig. 5 after four rounds of walking through paths A,A,B and A (Fig. 2b). Solid lines present the normalized prediction values for each mode while the dashed lines indicate the user switches and transitions from one mode to the next. It can be seen that upon transitions, the next intended mode had the higher prediction value than other modes, except for the current active mode, and that the trend of that prediction was ascending a few time-steps before the switching action, with some fluctuations.

#### IV. CONCLUSIONS AND DISCUSSION

This study demonstrated, for the first time, a proof of concept of GVF learning and prediction in lower-limb exoskeletons. Specifically, we demonstrated the application of a machine learning approach to reduce the burden on the users for manually switching between different available walking modes. Considering the two experimental scenarios in this work, an average decrease of 42.44% was seen in the total number of required switches, using the adaptive strategy in comparison to the best possible non-adaptive strategy. The techniques implemented in this work demonstrate a great potential for continuous real-time implementation of adaptive switching algorithms in lower-limb exoskeletons. The results showed that the purposed method was able to reduce the required switching actions noticeably in comparison to the best possible fixed switching list for each task, while using a single switch button. Using the adaptive switching approach, the target population can not only contain people with SCI (either complete or incomplete), but also be beneficial for people with other conditions such as stroke, multiple sclerosis or other groups who need assistance during walking. Moreover, the

core machine learning technology has also the capability and potential to be applied to other domains where generalities and similarities in the movements being performed are present.

There were some limitations in this study. The experiments were limited to the lab environment so the LiDAR sensors received noiseless signals. Also, the method used for determining the location of the user (although was only used offline and for verification purposes) cannot be applied to the real world, and high precision GPS systems are needed. Moreover, although limited walking modes were designed due to the restrictions of the lab environment, the system has the ability of predicting unlimited number of GVFs and re-ordering their respective walking modes in the switching list.

Future goals and next steps involve assessing the online capabilities of the machine learning system, designing less predictable experimental scenarios, utilizing more users and the addition of autonomous features to the system.

#### ACKNOWLEDGMENT

The authors thank Michel Gauthier and Adam Parker for their technical assistance and experiment-design consultation, respectively.

#### REFERENCES

- [1] W.-Z. Li, G.-Z. Cao, and A.-B. Zhu, "Review on Control Strategies for Lower Limb Rehabilitation Exoskeletons," *IEEE Access*, vol. 9, pp. 123040–123060, 2021, doi: 10.1109/ACCESS.2021.3110595.
- [2] J. de la Tejera, R. Bustamante-Bello, R. A. Ramirez-Mendoza, and J. Izquierdo-Reyes, "Systematic Review of Exoskeletons towards a General Categorization Model Proposal," *Appl. Sci.*, vol. 11, pp. 1–25, Dec. 2020, doi: 10.3390/app11010076.
- [3] L. Zhou, W. Chen, J. Wang, S. Bai, H. Yu, and Y. Zhang, "A Novel Precision Measuring Parallel Mechanism for the Closed-Loop Control of a Biologically Inspired Lower Limb Exoskeleton," *IEEEASME Trans. Mechatron.*, vol. 23, no. 6, pp. 2693–2703, Dec. 2018, doi: 10.1109/TMECH.2018.2872011.
- [4] M. R. Tucker *et al.*, "Control strategies for active lower extremity prosthetics and orthotics: a review," *J. NeuroEngineering Rehabil.*, vol. 12, no. 1, p. 1, 2015, doi: 10.1186/1743-0003-12-1.
- [5] R. Baud, A. R. Manzoori, A. Ijspeert, and M. Bouri, "Review of control strategies for lower-limb exoskeletons to assist gait," *J. NeuroEngineering Rehabil.*, vol. 18, no. 1, p. 119, Dec. 2021, doi: 10.1186/s12984-021-00906-3.
- [6] S. Qiu, W. Guo, D. Caldwell, and F. Chen, "Exoskeleton Online Learning and Estimation of Human Walking Intention Based on Dynamical Movement Primitives," *IEEE Trans. Cogn. Dev. Syst.*, vol. 13, no. 1, pp. 67–79, Mar. 2021, doi: 10.1109/TCDS.2020.2968845.
- [7] T. Vouga, R. Baud, J. Fasola, M. Bouri, and H. Bleuler, "TWIICE — A lightweight lower-limb exoskeleton for complete paraplegics," in *2017 International Conference on Rehabilitation Robotics (ICORR)*, London, Jul. 2017, pp. 1639–1645. doi: 10.1109/ICORR.2017.8009483.
- [8] X. Liu and Q. Wang, "Real-Time Locomotion Mode Recognition and Assistive Torque Control for Unilateral Knee Exoskeleton on Different Terrains," *IEEEASME Trans. Mechatron.*, vol. 25, no. 6, pp. 2722–2732, Dec. 2020, doi: 10.1109/TMECH.2020.2990668.
- [9] F. Xu, X. Lin, H. Cheng, R. Huang, and Q. Chen, "Adaptive stair-ascending and stair-descending strategies for powered lower limb exoskeleton," in *2017 IEEE International Conference on Mechatronics and Automation (ICMA)*, Takamatsu, Japan, Aug. 2017, pp. 1579–1584. doi: 10.1109/ICMA.2017.8016052.
- [10] H. A. Varol, F. Sup, and M. Goldfarb, "Powered sit-to-stand and assistive stand-to-sit framework for a powered transfemoral prosthesis," in *2009 IEEE International Conference on Rehabilitation Robotics*, Kyoto, Jun. 2009, pp. 645–651. doi: 10.1109/ICORR.2009.5209582.

- [11] X. Tan, B. Zhang, G. Liu, X. Zhao, and Y. Zhao, "Cadence-Insensitive Soft Exoskeleton Design With Adaptive Gait State Detection and Iterative Force Control," *IEEE Trans. Autom. Sci. Eng.*, pp. 1–14, 2021, doi: 10.1109/TASE.2021.3066403.
- [12] A. J. McDaid, Song Xing, and S. Q. Xie, "Brain controlled robotic exoskeleton for neurorehabilitation," in *2013 IEEE/ASME International Conference on Advanced Intelligent Mechatronics*, Wollongong, NSW, Jul. 2013, pp. 1039–1044. doi: 10.1109/AIM.2013.6584231.
- [13] J. Choi, K.-T. Kim, J. Lee, S. J. Lee, and H. Kim, "Robust Semi-synchronous BCI Controller for Brain-Actuated Exoskeleton System," in *2020 8th International Winter Conference on Brain-Computer Interface (BCI)*, Gangwon, Korea (South), Feb. 2020, pp. 1–3. doi: 10.1109/BCI48061.2020.9061658.
- [14] A. Kilicarslan, S. Prasad, R. G. Grossman, and J. L. Contreras-Vidal, "High accuracy decoding of user intentions using EEG to control a lower-body exoskeleton," in *2013 35th Annual International Conference of the IEEE Engineering in Medicine and Biology Society (EMBC)*, Osaka, Jul. 2013, pp. 5606–5609. doi: 10.1109/EMBC.2013.6610821.
- [15] J. Choi and H. Kim, "Real-time Decoding of EEG Gait Intention for Controlling a Lower-limb Exoskeleton System," in *2019 7th International Winter Conference on Brain-Computer Interface (BCI)*, Gangwon, Korea (South), Feb. 2019, pp. 1–3. doi: 10.1109/IWW-BCI.2019.8737311.
- [16] Y. He, D. Egreun, J. M. Azorín, R. G. Grossman, T. P. Luu, and J. L. Contreras-Vidal, "Brain-machine interfaces for controlling lower-limb powered robotic systems," *J. Neural Eng.*, vol. 15, no. 2, p. 021004, Apr. 2018, doi: 10.1088/1741-2552/aaa8c0.
- [17] W. Svensson and U. Holmberg, "Ankle-Foot-Orthosis Control in Inclinations and Stairs," in *2008 IEEE Conference on Robotics, Automation and Mechatronics*, Chengdu, China, Sep. 2008, pp. 301–306. doi: 10.1109/RAMECH.2008.4681479.
- [18] M. Sharifi, J. K. Mehr, V. K. Mushahwar, and M. Tavakoli, "Adaptive CPG-Based Gait Planning With Learning-Based Torque Estimation and Control for Exoskeletons," *IEEE Robot. Autom. Lett.*, vol. 6, no. 4, pp. 8261–8268, Oct. 2021, doi: 10.1109/LRA.2021.3105996.
- [19] S. C. Kirshblum *et al.*, "International standards for neurological classification of spinal cord injury (Revised 2011)," *J. Spinal Cord Med.*, vol. 34, no. 6, pp. 535–546, Nov. 2011, doi: 10.1179/204577211X13207446293695.
- [20] A. C. Villa-Parra *et al.*, "Control of a robotic knee exoskeleton for assistance and rehabilitation based on motion intention from sEMG," *Res. Biomed. Eng.*, vol. 34, no. 3, pp. 198–210, Jul. 2018, doi: 10.1590/2446-4740.07417.
- [21] P. T. Chinimilli, S. C. Subramanian, S. Redkar, and T. Sugar, "Human Locomotion Assistance using Two-Dimensional Features Based Adaptive Oscillator," in *2019 Wearable Robotics Association Conference (WearRAcon)*, Scottsdale, AZ, USA, Mar. 2019, pp. 92–98. doi: 10.1109/WEARRACON.2019.8719628.
- [22] F. Cordella *et al.*, "Literature Review on Needs of Upper Limb Prosthesis Users," *Front. Neurosci.*, vol. 10, May 2016, doi: 10.3389/fnins.2016.00209.
- [23] M. Liu, D. Wang, and H. Huang, "Development of an Environment-Aware Locomotion Mode Recognition System for Powered Lower Limb Prostheses," *IEEE Trans. Neural Syst. Rehabil. Eng.*, vol. 24, no. 4, pp. 434–443, Apr. 2016, doi: 10.1109/TNSRE.2015.2420539.
- [24] S. Carvalho, J. Figueiredo, and C. P. Santos, "Environment-Aware Locomotion Mode Transition Prediction System," in *2019 IEEE International Conference on Autonomous Robot Systems and Competitions (ICARSC)*, Porto, Portugal, Apr. 2019, pp. 1–6. doi: 10.1109/ICARSC.2019.8733658.
- [25] N. E. Krausz and L. J. Hargrove, "Recognition of ascending stairs from 2D images for control of powered lower limb prostheses," in *2015 7th International IEEE/EMBS Conference on Neural Engineering (NER)*, Montpellier, France, Apr. 2015, pp. 615–618. doi: 10.1109/NER.2015.7146698.
- [26] B. Laschowski, W. McNally, A. Wong, and J. McPhee, "Preliminary Design of an Environment Recognition System for Controlling Robotic Lower-Limb Prostheses and Exoskeletons," in *2019 IEEE 16th International Conference on Rehabilitation Robotics (ICORR)*, Toronto, ON, Canada, Jun. 2019, pp. 868–873. doi: 10.1109/ICORR.2019.8779540.
- [27] R. J. Farris, H. A. Quintero, and M. Goldfarb, "Preliminary Evaluation of a Powered Lower Limb Orthosis to Aid Walking in Paraplegic Individuals," *IEEE Trans. Neural Syst. Rehabil. Eng.*, vol. 19, no. 6, pp. 652–659, Dec. 2011, doi: 10.1109/TNSRE.2011.2163083.
- [28] H. A. Quintero, R. J. Farris, C. Hartigan, I. Clesson, and M. Goldfarb, "A Powered Lower Limb Orthosis for Providing Legged Mobility in Paraplegic Individuals," *Top. Spinal Cord Inj. Rehabil.*, vol. 17, no. 1, pp. 25–33, 2011, doi: 10.1310/sci1701-25.
- [29] M. Sharifi, J. K. Mehr, V. K. Mushahwar, and M. Tavakoli, "Autonomous locomotion trajectory shaping and nonlinear control for lower-limb exoskeletons," *IEEE/ASME Trans. on Mechatronics*, Published online, 2022.
- [30] J. K. Mehr, M. Sharifi, V. K. Mushahwar, and M. Tavakoli, "Intelligent Locomotion Planning With Enhanced Postural Stability for Lower-Limb Exoskeletons," *IEEE Robot. Autom. Lett.*, vol. 6, no. 4, pp. 7588–7595, Oct. 2021, doi: 10.1109/LRA.2021.3098915.
- [31] D. R. Louie, J. J. Eng and T. Lam, "Gait speed using powered robotic exoskeletons after spinal cord injury: a systematic review and correlational study," *J. Neural Eng.*, 2015, doi: 10.1186/s12984-015-0074-9
- [32] S. Richard *et al.*, "Horde : A Scalable Real-time Architecture for Learning Knowledge from Unsupervised Sensorimotor Interaction," *Proc. 10th Int. Conf. Auton. Agents Multiagent Syst.*, pp. 761–768, 2011.
- [33] A. White, "Developing a Predictive Approach to Knowledge," 2015, doi: 10.7939/R3FF3M75H.
- [34] J. Modayil, A. White, and R. S. Sutton, "Multi-timescale Nexting in a Reinforcement Learning Robot," *ArXiv11121133 Cs*, Jun. 2012, Accessed: Feb. 15, 2022. [Online]. Available: <http://arxiv.org/abs/1112.1133>
- [35] P. M. Pilarski *et al.*, "Adaptive artificial limbs: a real-time approach to prediction and anticipation," *IEEE Robot. Autom. Mag.*, vol. 20, no. 1, pp. 53–64, Mar. 2013, doi: 10.1109/MRA.2012.2229948.
- [36] P. M. Pilarski, M. R. Dawson, T. Degris, J. P. Carey, and R. S. Sutton, "Dynamic switching and real-time machine learning for improved human control of assistive biomedical robots," in *2012 4th IEEE RAS & EMBS International Conference on Biomedical Robotics and Biomechatronics (BioRob)*, Rome, Italy, Jun. 2012, pp. 296–302. doi: 10.1109/BioRob.2012.6290309.
- [37] A. L. Edwards *et al.*, "Application of real-time machine learning to myoelectric prosthesis control: A case series in adaptive switching," *Prosthet. Orthot. Int.*, vol. 40, no. 5, pp. 573–581, Oct. 2016, doi: 10.1177/0309364615605373.
- [38] A. L. Edwards, J. S. Hebert, and P. M. Pilarski, "Machine learning and unlearning to autonomously switch between the functions of a myoelectric arm," in *2016 6th IEEE International Conference on Biomedical Robotics and Biomechatronics (BioRob)*, Singapore, Singapore, Jun. 2016, pp. 514–521. doi: 10.1109/BIOROB.2016.7523678.
- [39] J. B. Travník and P. M. Pilarski, "Representing high-dimensional data to intelligent prostheses and other wearable assistive robots: A first comparison of tile coding and selective Kanerva coding," in *2017 International Conference on Rehabilitation Robotics (ICORR)*, London, Jul. 2017, pp. 1443–1450. doi: 10.1109/ICORR.2017.8009451.
- [40] A. N. Dalrymple, D. A. Roszko, R. S. Sutton, and V. K. Mushahwar, "Pavlovian control of intraspinal microstimulation to produce over-ground walking," *J. Neural Eng.*, vol. 17, no. 3, p. 036002, Jun. 2020, doi: 10.1088/1741-2552/ab8e8e.
- [41] S. P. Singh and R. S. Sutton, "Reinforcement Learning with Replacing Eligibility Traces," *Mach. Learn.*, vol. 22, no. 1/2/3, pp. 123–158, 1996, doi: 10.1023/A:1018012322525.
- [42] R. S. Sutton and A. G. Barto, *Reinforcement Learning, second edition: An Introduction*. MIT Press, 2018.